Media Effects on the Mechanism of Antioxidant Action of Silybin and 2,3-Dehydrosilybin: Role of the Enol Group

3 **AUTHORS**, INCLUDING:

Grzegorz Litwinienko
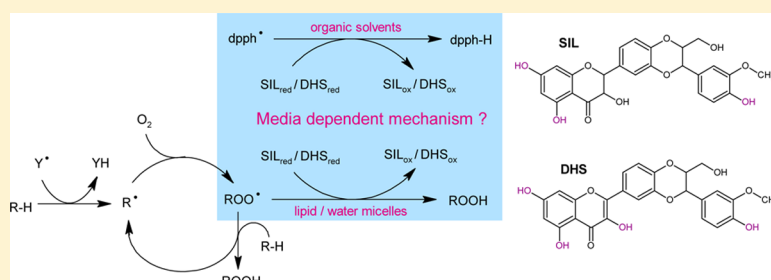University of Warsaw

51 PUBLICATIONS   **1,657** CITATIONS

Media Effects on the Mechanism of Antioxidant Action of Silybin and 2,3-Dehydrosilybin: Role of the Enol Group

Ewelina van Wenum, Rafal Jurczakowski, and Grzegorz Litwinienko*

University of Warsaw, Faculty of Chemistry, Pasteura 1, 02-093 Warsaw, Poland

Ⓢ Supporting Information

ABSTRACT: Silybin (SIL) and 2,3-dehydrosilybin (DHS) are constituents of milk thistle extract (silymarin) applied in the treatment of cirrhosis, hepatitis, and alcohol-induced liver disease. The molecular mechanism of their action is usually connected with antioxidant action. However, despite experimental and theoretical evidence for the antioxidant activity of SIL and DHS, the mechanism of their antiradical action still remains unclear. We studied the kinetics of SIL/DHS reactions with 2,2-diphenyl-1-picrylhydrazyl radical in organic solutions of different polarity and with peroxyl radicals in a micellar system mimicking the amphiphilic environment of lipid membranes. Kinetic studies together with determination of acidity and electrochemical measurements allowed us to discuss the structure−activity relationship in detail. In nonpolar solvents the reaction with free radicals proceeds via a one-step hydrogen atom transfer (HAT) mechanism, while significant acceleration of the reaction rates in methanol and water/methanol solutions suggests the dominating contribution of a sequential proton-loss electron-transfer (SPLET) mechanism with participation of the most acidic hydroxyl groups: 7-OH in SIL and 7-OH and 3-OH in DHS. In a heterogeneous water/lipid system, both mechanisms operate; however, the reaction kinetics and the antioxidant efficacy depend on the partition between lipid and water phases.

■ INTRODUCTION

The vast majority of presently applied medicines are of natural origin[1−3] with such evident examples as aspirin,[4] morphine,[5] quinine,[6] noscapine,[7] curcumin,[8] and digitalis.[9] According to the WHO, up to 80% of population relies currently on traditional remedies. Echinacea, ginko, ginseng, garlic, St. John's wort, milk thistle, and valerian[10,11] are just a few examples of herbs used commonly, regardless of the uncertainty of the formulation, incomplete studies of individual and cooperative mechanisms of action of all constituents, and insufficient amount of reliable clinical trials.[1,11,12] Milk thistle (*Silybum marianum* (L.) Gaertn.) is a herbaceous plant that has been used in folk medicine since ancient times, mainly in the treatment of various liver disorders. Nowadays, the most common indications for administration of milk thistle extract (i.e., silymarin) are cirrhosis, acute and chronic hepatitis, alcohol-induced liver disease, and toxin-induced hepatitis.[13−18] It is widely applied due to its safety and lack of adverse effects. Contemporary research has broadened the knowledge about its hepato- and cardioprotective properties, anticholestatic, anticancer, and antimetastatic efficacy, as well as neuroactive and neuroprotective activity.[19−22] With a few exceptions, the increasing amount of knowledge on the health benefits has not been accompanied by comprehensive basic research on the molecular mechanisms of action.

Scheme 1. Chemical Structures of Silybin (A) and 2,3-Dehydrosilybin (B)
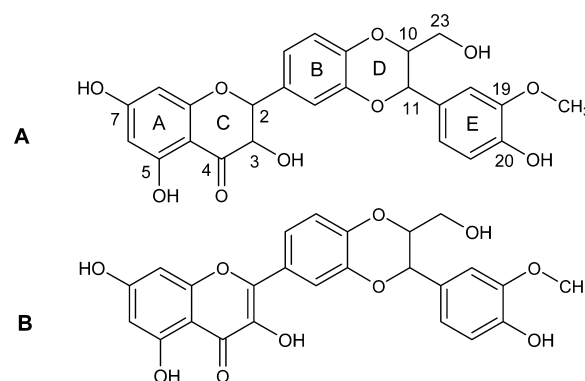
Silybin (SIL, Scheme 1A), as the main constituent of silymarin, is considered to exhibit the foremost biological activity. Among a number of intracellular mechanisms responsible for the activity of SIL, antioxidant action appears to be the key mechanism.[18,23−29] Other documented mechanisms include stimulation of polymerase I,

rRNA transcription,[30] stabilization of cellular membrane and regulation of its permeability to protect the cells against xenobiotics.[31−33] The composition of silymarin includes also other flavonolignans (such as 2,3-dehydrosilybin, isosilybin, silychristin, and silydianin) and some flavonoids (taxifolin, quercetin). The rest (10−30%) of the extract is a chemically undefined fraction containing some other polyphenolic compounds.[23] 2,3-Dehydrosilybin (DHS, Scheme 1B) has received special attention only recently, since, in comparison to SIL, it is a 25 times more potent radical scavenger and inhibits lipid peroxidation 10 times more efficiently.[26,34]

Silymarin and silybin have been intensively studied in vitro, in vivo, and also in clinical trials.[35] However, only a few papers have provided insight into their structure−activity relationship. Gyorgy et al.[36] indicated the 20-OH group in silybin as the most probable site of hydrogen atom abstraction by free radicals. Gažák et al.[25] investigated the role of individual hydroxyl groups in silybin, 2,3-dehydrosilybin, and their methylated derivatives on the basis of reaction with 2,2-diphenyl-1-picrylhydazyl radical (dpph•) in methanol solution, the inhibition effect of these flavolignans on microsomal lipid peroxidation, and on superoxide scavenging in the mitochondria from brown adipose tissue (BAT). The authors concluded that the phenolic 20-OH group is responsible for the antiradical activity of SIL, while for DHS the most important group is enolic 3-OH, with a smaller contribution of the 20-OH group to the overall reactivity.

There are several thermodynamic and kinetic factors governing the mechanism of reaction of chain-breaking phenolic antioxidants (ArOH) with free radicals (Y•):[37,38] the structure of ArOH, the O−H bond dissociation enthalpy ($BDE_{O−H}$), the ionization potential (IP) and acidity of ArOH, the reactivity and electron affinity of Y•, and some external factors such as reaction environment, including polarity of a solvent, its ability to form a hydrogen bond, pH,[39] the structure of the membrane, and the presence of coantioxidants. Hydrogen atom transfer (HAT) and proton-coupled electron transfer (PCET)[40,41] are examples of a one-step mechanism.[42] Other mechanisms include separable steps of electron/proton transfer. In the sequential proton-loss electron-transfer mechanism (SPLET)[43−45] a deprotonation precedes the electron transfer from phenolate anion to a radical and this mechanism clearly depends on the ability of a solvent to support ionization, acidity of a phenol, and electron affinity of a radical.[41] Another mechanism, electron transfer−proton transfer (ET-PT), includes the opposite order of steps: electron transfer from a phenol gives a radical cation that immediately deprotonates to form phenoxyl radical.

The mechanisms of action of silybin and 2,3-dehydrosilybin were theoretically studied by Trouillas et al.[23] The authors concluded that due to a low $BDE_{O−H}$ value in DHS the 3-OH and 20-OH groups are able to participate in HAT, whereas for silybin, having relatively stronger O−H bonds, other mechanisms, namely electron transfer (ET) and formation of adducts with radicals, are more probable. Very recently, the same authors[46] have suggested that the 7-OH group may react via the SPLET mechanism in a way similar to that described by Musialik et al.[47] for 7-OH groups in other flavonoids. However, despite experimental[18,24−29,35,36] and theoretical[23] evidence of the antioxidant activity of SIL and DHS, the mechanism of their antiradical action still remains unclear. In this work we describe the kinetics of their reaction with model dpph• radical in homogeneous solutions and with lipid peroxyl radicals in heterogeneous systems. The results are combined with the acidity of these two flavolignans, and on the basis of such structure−activity relationships we propose the mechanisms of antiradical action of SIL and DHS.

■ RESULTS AND DISCUSSION

Acidity of Hydroxyl Groups. The acidities of SIL and DHS were determined by spectrophotometric titration in water/methanol (1/1) with the same methodology as previously used for other flavonoids.[47] The UV−vis plots recorded during titration are presented in the Supporting Information. The obtained values are in good agreement with previous studies on the acidity of flavonoids.[47−49]

Acidity of SIL. The pK_a values determined for SIL are 7.7 ± 0.06 and 11.0 ± 0.08. Meloun et al.[50] reported four pK_a values for silybin: 7.00, 8.77, 9.57, and 11.66, corresponding to three phenolic and one nonphenolic OH group. However, pK_a = 11.66 reported for nonphenolic OH is inconsistent with the values usually expected for aliphatic alcohols (15.5−18 in water).[51] In our measurements we focused on the ionization of phenolic groups. The number of ionization steps determined by us is lower than the number of phenolic groups in SIL by one. To understand this difference, we decided to assign pK_a values to particular OH groups, on the basis of structural similarities to other compounds of known acidities (Scheme 2).

Scheme 2. Structures of Phenols with Their pK_a Values Taken from the Literature (As Cited): (A) 6-Hydroxy-1-tetralone;[52] (B) 4-Hydroxyacetophenone;[53] (C) 2-Methoxyphenol (Guaiacol);[43] (D) 5,7-Dihydroxyflavone (Chrysin);[47] (E) 3,5,7-Trihydroxyflavone (Galangin);[47] (F) SIL (This Work); (G) DHS (This Work)
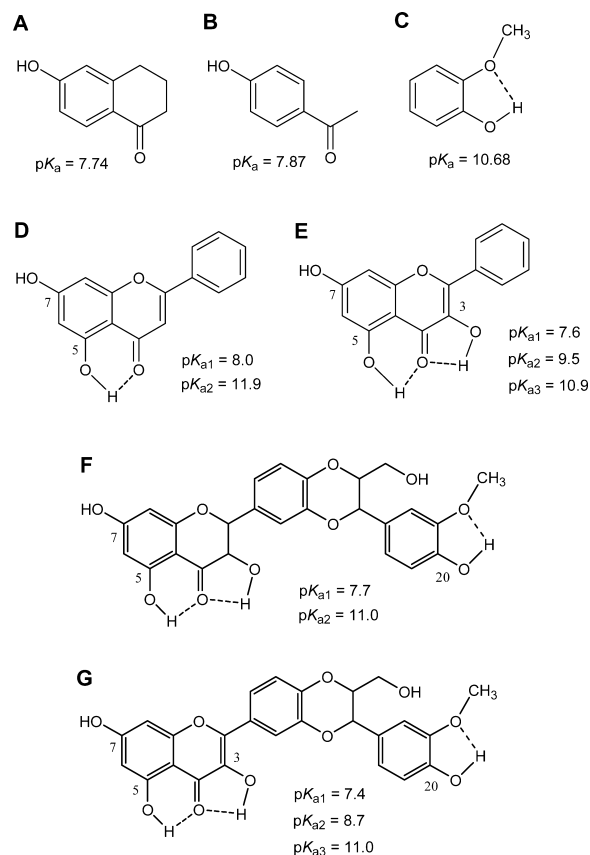
In SIL, a phenolic OH at position 20 is internally H-bonded to an o-methoxyl group. Since ring E is not conjugated with other rings, the acidity of 20-OH should be similar to the acidity of guaiacol (see Scheme 2C, pK_a = 10.68 in water[43]); thus, pK_{a2} can be assigned to the 20-OH group. Two other

phenolic OH groups in SIL are at positions 5 and 7 in ring A. A detailed discussion about the acidity of hydroxyflavones[47] showed that 7-OH groups are the most acidic, regardless of the hydroxylation pattern, with pK_a values between 7.5 and 8.5. Also, the phenols presented in Scheme 2A,B, resembling structurally a part of the SIL molecule, have pK_a's of 7.74 and 7.87, respectively. All of these values suggest that the pK_{a1} for SIL (7.7) can be ascribed to the 7-OH group. After the 7-OH group is ionized, the remaining 5-OH group (H-bonded to the adjacent carbonyl group) is nonionized until the pH reaches 11, as for other flavones with OH groups at positions 5 and 7; see the structures and pK_a values for chrysin and galangin in Scheme 2D,E. That is, both groups, 5-OH and 20-OH, deprotonate at the same pH region and the processes cannot be deconvoluted.

Acidity of DHS. The pK_a values obtained for DHS are 7.4 ± 0.10, 8.7 ± 0.09, and 11.0 ± 0.05. pK_{a1} and pK_{a3} for DHS correspond very well to pK_a values obtained for SIL and, considering the structural similarity between SIL and DHS, they might be assigned to the same phenolic groups in both flavolignans. The presence of a double bond between C2 and C3 in DHS causes a rather small (less than $^1/_2$ unit) decrease of pK_{a1}, leaving the pK_{a3} value practically unchanged, in comparison to SIL. More importantly, it changes the character of the 3-OH group from alcohol (in SIL) to enol (in DHS).[43] This causes a major shift in pK_a value for the hydroxyl group: from very high, characteristic for aliphatic alcohols (vide supra), to $pK_{a2} = 8.7$.

Kinetics of the Reaction with dpph•. The reaction of a phenolic chain-breaking antioxidant with a free radical can be represented by the overall process (1) with the mechanism depending mainly on the structure of ArOH, polarity of microenvironment, localization and ionization of the antioxidant.

$$Y^\bullet + ArOH \xrightarrow{k_{inh}} YH + ArO^\bullet \tag{1}$$

For a simple HAT process in H-bond (HB) accepting solvents (S), the formation of the hydrogen bond ArO—H···S causes steric hindrance leading to inaccessibility of phenolic OH for radicals. This phenomenon, called the Kinetic Solvent Effect (KSE), was quantitatively described by Ingold et al.:[54]

$$\log(k^S/M^{-1}s^{-1}) = \log(k^\circ/M^{-1}s^{-1}) - 8.3\alpha_2^H\beta_2^H \tag{2}$$

where k^S is the overall bimolecular rate constant of the reaction carried out in an HB-accepting solvent, k° is the rate constant of the process carried out in a non-HB-accepting solvent, and the parameters α_2^H and β_2^H describe the HB-donating ability of a phenol and HB-accepting ability of a solvent, respectively. Both parameters range from 0.0 to 1.0, and their values are accessible for hundreds of compounds.[55,56] Equation 2 predicts that any HAT process occurring in HB-accepting solvent ($\beta_2^H > 0$) is always slower than in hydrocarbons ($\beta_2^H = 0$), in agreement with a large number of experimental results.[57,58]

The rate constants k^S measured for the processes carried out in ionization-supporting solvents (such as methanol, ethanol, and water) are usually greater than predicted by eq 2. Such an increase of k^S is due to the participation of the SPLET mechanism (reactions 3−5),[59] with very fast electron transfer

$$ArOH \leftrightarrows ArO^- + H^+ \tag{3}$$

$$ArO^- + Y^\bullet \rightarrow ArO^\bullet + Y^- \tag{4}$$

$$Y^- + H^+ \leftrightarrows HY \tag{5}$$

from the phenolate anion to a radical (reaction 4). The SPLET mechanism was originally proposed for phenols (even for

as weak acids as butylated hydroxytoluene and tocopherol)[60] reacting with electron-deficient radicals (e.g., dpph•) in ionization-supporting solvents. For HAT processes there is a relationship between the rate constants $k_{ArOH/dpph}$• and $k_{ArOH/ROO}$• (where ROO• denotes peroxyl radical);[61] thus, the stable dpph• radical is frequently applied as a simple model of peroxyl radicals[62] for studies of the structure−activity relationship for many antioxidant systems. The conclusions, if carefully interpreted, can be applied in oxidative processes involving peroxyl radicals as reactive intermediates.

We measured bimolecular rate constants k^S for reaction 6 carried out in 1,4-dioxane ($\beta_2^H = 0.41$ (0.47);[55,63] $\varepsilon = 2.2$), ethyl

$$dpph^\bullet + ArOH \xrightarrow{k^S} dpph\text{-}H + ArO^\bullet \tag{6}$$
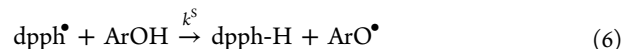
acetate (AcOEt, $\beta_2^H = 0.45$;[55] $\varepsilon = 6.0$), and methanol ($\beta_2^H = 0.41$;[55] $\varepsilon = 32$). Analysis of data collected in Table 1 shows that with increasing solvent polarity (dioxane < AcOEt < methanol) an enormous acceleration of reaction 6 occurs: 200-fold for SIL and 1300-fold for DHS. Similar β_2^H parameters for dioxane,[63] ethyl acetate, and methanol ensure the same magnitude of KSE; therefore, this huge acceleration of k^S can be interpreted as a result of a SPLET contribution.[41] A significant decrease of k^S values (ca. 15 and 140 times for SIL and DHS, respecively) after the addition of acetic acid ($\beta_2^H = 0.42$)[58] to methanol is additional proof of the SPLET participation in the overall process. Such a dramatic difference between k^{MeOH} and k^{MeOH/H^+} can be assigned to a very small amount of ionized phenols in the presence of stronger acid; thus, the k^{MeOH/H^+} values are similar to k^{AcOEt}.

Reaction Sites in SIL. There are three phenolic groups in the SIL molecule (Scheme 3). Since the 20-OH group has the lowest BDE,[23] it has been reported as the most reactive site in HAT.[25] Other phenolic groups have higher BDEs, and their input to SIL's activity is considerably smaller. We compared the reactivity of SIL with the reactivity of 2-methoxyphenol (guaiacol; see the structure in Scheme 2C), a molecule structurally similar to ring E in SIL. Values of the rate constants collected in Table 1 for guaiacol/dpph• reactions are similar to the results for SIL in the same solvents, suggesting a dominating contribution of the 20-OH group to the overall activity of SIL. Another part of the SIL molecule (ACB rings, see Scheme 1) is structurally similar to 5,7-dihydroxyflavone (chrysin; see Scheme 2D), with the same hydroxylation pattern (3-OH in SIL is an alcohol group and is not taken into consideration) and very similar acidities. The rate constants determined for dpph•/chrysin in dioxane and ethyl acetate (Table 1) are considerably smaller than for dpph•/guaiacol in the same solvents, suggesting small activity of 5- and 7-OH groups in HAT, consistent with their high BDEs (89.8 and 103.6 kcal/mol, respectively[64]). The comparison of reactivity of SIL with the reactivities of its two building blocks, guaiacol and chrysin, gives a strong argument for the dominating role of 20-OH as a main site of hydrogen atom abstraction from SIL.

However, for reactions carried out in methanol (a solvent supporting the ionization), SIL, chrysin, and guaiacol react with dpph• considerably faster than in dioxane and in acidified methanol (see Table 2), indicating an increasing role of electron transfer from phenolate anions to dpph• in the overall reaction kinetics. Two parts of the SIL molecule, depending on their acidity and BDE values, can react with dpph• radicals with two independent mechanisms. The most acidic 7-OH group in ring A reacts via the SPLET mechanism (because the O−H bond

Table 1. Bimolecular Rate Constants k^S for Reactions of dpph[•] with SIL, DHS, and Structurally Related (Poly)phenols and the Ratio k^s(DHS)/k^s(SIL) in Organic Solvents and Two Buffered Systems

	k^S (M^{-1} s^{-1})[a]					
solvent	SIL	DHS	guaiacol	chrysin[b]	galangin[b]	k^S(DHS)/k^S(SIL)
dioxane	0.030	0.21	0.055[c]	0.0030	0.27	7
AcOEt	0.11	2.85	0.14[c]	0.074	0.62	26
methanol	6.5	273	7.8	2.7	310	42
acidified methanol[d]	0.47	1.9	0.12	0.15[e]	3.4	4
acetic buffer pH 5.5[f,g]	19	188	nd	nd	nd	10
Tris buffer pH 7.4[f,g]	28	604	nd	nd	nd	21

[a]With errors ±20%. [b]Reference 47; see structures D and E in Scheme 2. [c]Reference 43. [d]Containing 100 mM acetic acid. [e]Containing 10 mM acetic acid. [f]In a water/methanol system (1/1). [g]nd = not determined.

Scheme 3. Experimental Values of pK$_a$ (Our Measurements) and Theoretical Values of BDE's in the Gas Phase and in Polar Solvent (in kcal/mol) for SIL and DHS[a]
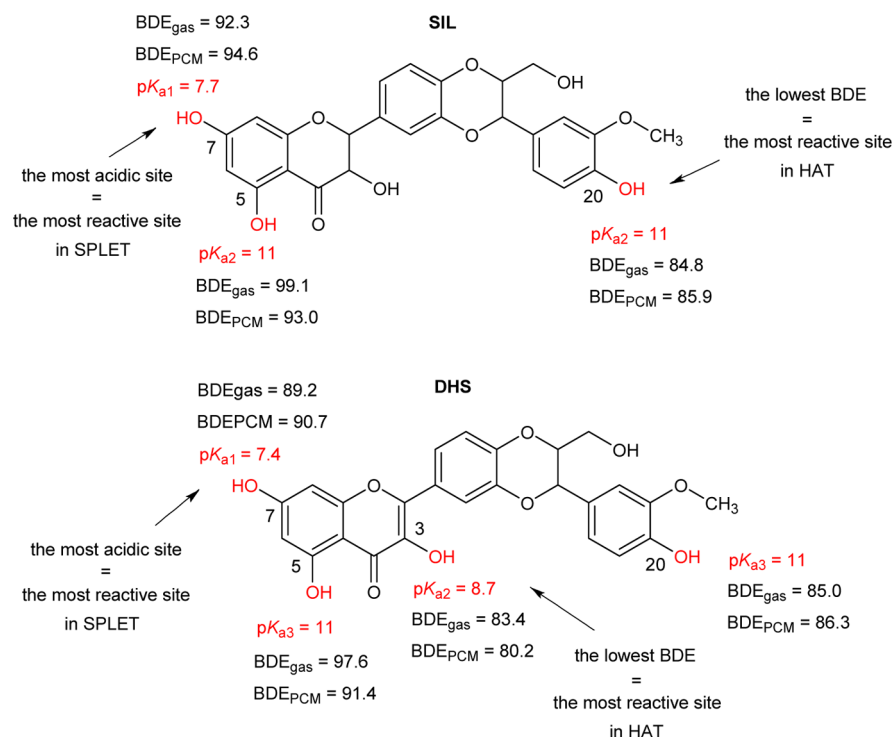
[a]BDE parameters were taken from Trouillas et al.[23]

Table 2. Acceleration Ratios

|	$k^{MeOH}/k^{dioxane}$	$k^{MeOH}/k^{MeOH/H^+}$ [a]
SIL	217	14
chrysin[b]	900	18[c]
DHS	1300	144
galangin[b]	1148	91
guaiacol	144	66

[a]MeOH/H$^+$ containing 100 mM acetic acid. [b]Reference 47. [c]MeOH/H$^+$ containing 10 mM acetic acid.

is too strong to undergo HAT; vide supra) to give a phenoxyl radical with an electron delocalized over ring A of the SIL molecule (path **I → III → IV**, Scheme 4), whereas the 20-OH site (with the lowest BDE and much higher pK$_a$) reacts via the HAT mechanism (path **I → II**). Although data in Table 2 suggest that guaiacol can also participate in SPLET, this is not the case for the 20-OH group, because the presence of more acidic groups in the same system (such as 7-OH in SIL) shifts

back the deprotonation of the very weakly acidic 20-OH to make it fully protonated.

Reaction Sites in DHS. In comparison to SIL, the only structural difference in DHS is the presence of a C2−C3 double bond, leading to two important consequences: a change in the chemical character of the 3-OH group from alcoholic (in SIL) to enolic (in DHS) and conjugation of rings A, C, and B. The importance of the 3-OH group conjugated with the C2−C3 double bond and adjacent carbonyl group in flavonoids has been emphasized in the literature.[26,47,65] However, there is much controversy about the conjugation of rings in flavones, with some theoretical[66] and experimental[67] reports on the lack of aromatic character of ring C in chromone, whereas other works claim the aromaticity of the entire molecule of chromone.[68] Introduction of the 3-OH group to form 3-hydroxyflavone causes increased aromaticity of the pyrone ring.[69] Also, ring B is considered as conjugated with the 3-OH group in flavone.[70] Trouillas and co-workers[71,72] demonstrated that hydroxyflavones with a C4 keto group, 3-OH group and C2−C3 double bond do exhibit π

Scheme 4. Mechanism of Reaction of Silybin with Free Radicals in Polar Solvents
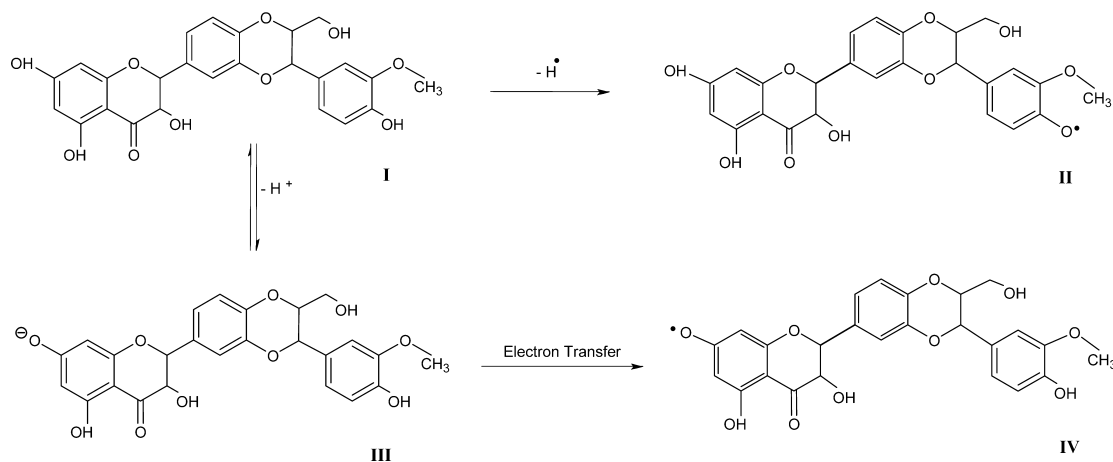
Scheme 5. Mechanism of Reaction of 2,3-Dehydrosilybin with Free Radicals in Polar Solvents
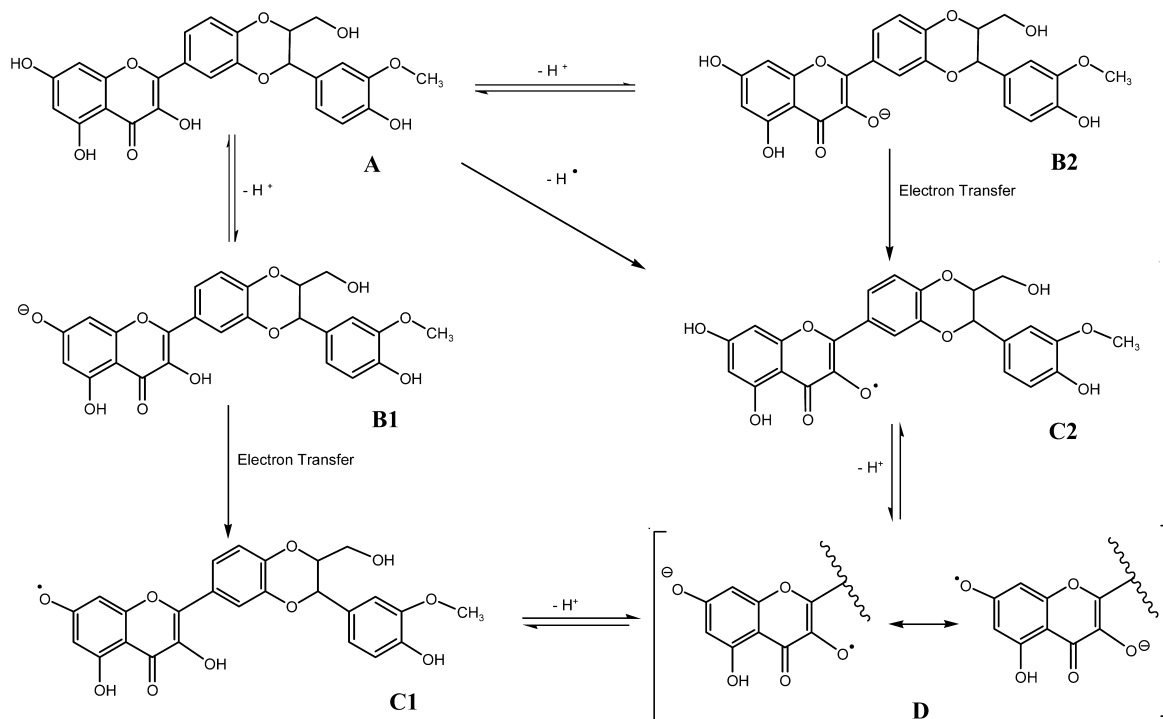
conjugation over the entire molecule (e.g., galangin, quercetin); removal of 3-OH (as in chrysin or luteolin) leads to partial loss of π conjugation, while lack of the C2–C3 double bond (as in taxifolin) interrupts the conjugation path. The extended electron delocalization in hydroxyflavones has also been highlighted by many other authors.[23,47,73−79] In DHS the planarity of the whole system of rings A, C, and B permits the conjugation[23] and the OH groups at positions 3, 5, and 7 in the flavone structure form an optimal hydroxylation pattern for the antioxidant activity of rings A and C.[65]

The results collected in Tables 1 and 2 clearly show that DHS scavenges dpph[•] radicals 4−40 times faster than SIL does, depending on the solvent. Such enhanced reactivity of DHS cannot be assigned to the 20-OH group (present in both, SIL and DHS); therefore, the hydroxylation pattern in rings A and C appears to be responsible for the fast reaction with dpph[•]. The BDE value for enolic 3-OH is 1.6 kcal/mol lower than for 20-OH in DHS and 1.4 kcal/mol lower than for 20-OH in SIL

(gas phase).[23] Thus, the presence of 3-OH together with 20-OH results in better reactivity of DHS (compared to SIL) in dioxane and in acidified methanol.

The enormously large acceleration of DHS/dpph[•] reaction in methanol can be ascribed directly to the ACB part of the DHS molecule, because other parts of DHS and SIL are identical. Galangin (3,5,7-trihydroxyflavone; Scheme 2E) is an excellent model for this part of DHS, and we found a very satisfactory agreement between the kinetic data obtained for DHS and for galangin (Tables 1 and 2) in all studied solvents. Additionally, comparison of k^S values obtained for DHS with those obtained for galangin (identical with rings A, C, and B in DHS) and guaiacol (identical with ring E in DHS) and for SIL (lacking only the enolic character of 3-OH) indicates that the enolic 3-OH group is very important, regardless of the change in the mechanism of action when passing from nonpolar to polar solvents. Therefore, in methanol the most acidic groups of DHS (7-OH and 3-OH) undergo deprotonation followed by

fast electron transfer (paths $A \rightarrow B1 \rightarrow C1$ and $A \rightarrow B2 \rightarrow C2$ in Scheme 5). Due to the presence of the strongly electron withdrawing character of $O^{\bullet}$,[43] the hydroxyl groups in the radicals **C1** and **C2** are prone to deprotonation, leading to the formation of **D**. Of course, the HAT mechanism is also possible, due to the low BDE of 3-OH in water,[23] and it should not be excluded in polar solvents (path $A \rightarrow C2$ in Scheme 5).

Reactions in Buffered Water/Methanol Solutions. We also measured k^S values for reactions of dpph$^{\bullet}$ with SIL and DHS carried out in water/methanol (1/1) buffered solutions (Table 1). The increase of pH from 5.5 to 7.4 causes an increase of k^S: from 17 to 28 M^{-1} s^{-1} for SIL and from 190 to 600 M^{-1} s^{-1} for DHS. These results corroborate the SPLET mechanism; however, the observed acceleration is lower than would be expected on the basis of the increased fraction of ionized phenol (50-fold increase for SIL). This apparent contradiction may be explained by the formation of a relatively unstable radical after electron transfer from the phenolate anion (i.e., from deprotonated 7-OH in ring A of SIL). The radical is not stable enough to efficiently shift the equilibrium of the reaction 4 (dpph$^{\bullet}$ + phenoate^{-} $\rightleftarrows$ dpph^{-} + phenoxyl$^{\bullet}$) toward the products. Thus, the 20-OH group is still the most reactive site in the reaction of SIL with dpph$^{\bullet}$ (the HAT mechanism dominates over the SPLET mechanism, regardless of the ionization of the 7-OH group). In DHS, the presence of the C2−C3 double bond together with the enolic 3-OH group makes an additional conjugation of rings A, C, and B, and thus, the acceleration of the DHS/dpph$^{\bullet}$ reaction is more sensitive toward increasing pH. At pH 7.4 about 46% of 7-OH (less reactive) and 2.6% of 3-OH (more reactive) groups are deprotonated. The ionization of the 3-OH group (as the more reactive site of SPLET) correctly explains the 3-fold increase of overall k^S when the pH is changed from 5.5 to 7.4, because this new reactive site dominates over the reactivity of the 20-OH group (which still operates via the HAT mechanism).

Cyclic Voltammetry of SIL and DHS. The electrochemical behavior of SIL and DHS was investigated by cyclic voltammetry over a pH range of 4−10, and typical voltammograms obtained at pH 4.0 are shown in Figure 1A. For SIL we observed two anodic peaks (E_2 and E_3) within the whole pH range, but for DHS three peaks (E_1, E_2, and E_3) at low pH's and four peaks (E_{1a}/E_{1b}, E_2, and E_3) at high pH's can be detected.

Trouillas et al.[23] interpreted cyclic voltammograms recorded at pH 7.0. Selective methylation of SIL and DHS allowed the authors to assign the E_1 peak to the oxidation of the 3-OH group in DHS and the E_2 peak to the oxidation of the 20-OH group in SIL. Gyorgy et al.[80] also ascribed the first oxidation peak for SIL to the oxidation of the 20-OH group. In our measurements performed at two different scan rates, 5 mV s^{-1} (resembling equilibrium conditions) and 50 mV s^{-1} (see the Supporting Information), we detected no substantial kinetic limitations for electrooxidation of SIL and DHS. At a scan rate of 5 mV s^{-1} both compounds exhibit E_2 peaks at very similar potentials within the whole pH range (Figure 1B), and hence the E_2 peak can be ascribed to the oxidation of the 20-OH group also in DHS. The E_1 peak is found for DHS only; thus, we confirm the assignment of the E_1 peak to the oxidation of the 3-OH site. The E_1, E_2, and E_3 peaks were recorded for the first scan only, and no oxidation current was detected for subsequent scans, indicating that the electrode surface became entirely blocked. Hence, the E_3 peak is most probably related to the oxidation of products formed after the electrochemical steps (E_1, E_2) and cannot be assigned to any phenolic group in SIL/DHS.
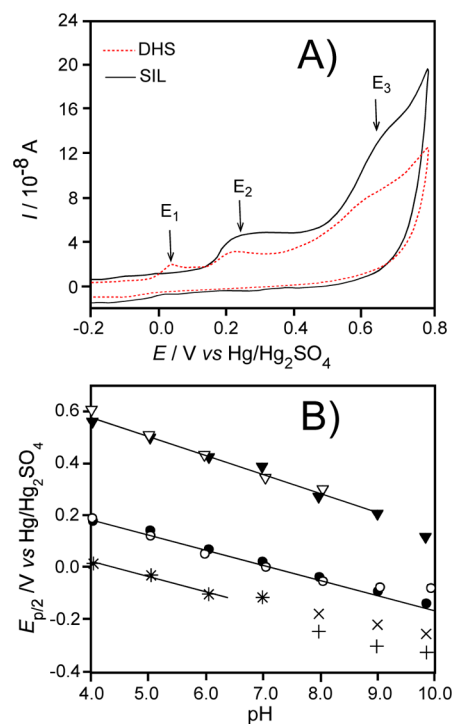

Figure 1. (A) Cyclic voltammograms for SIL and DHS recorded at pH 4.0 (scan rate 5 mV s^{-1}) with marked peaks E_1, E_2, and E_3. (B) $E_{p/2}$ values for DHS (E_1, *; E_{1a}, +; E_{1b}, ×; E_2, ●; E_3,▼) and for SIL (E_2, ○; E_3, ▽) determined over the pH range 4.0−10.0.

There are many internal and external features contributing to the antioxidant activity, and one of the most important is the ability of an antioxidant molecule to be a reducing agent. This mechanistically very important property can be parametrized by the half-peak oxidation potential ($E_{p/2}$).[65,81] Van Acker et al.[81] proposed a classification of radical scavengers, depending on their $E_{p/2}$ values vs a saturated calomel reference electrode (SCE): good ($E_{p/2} < 0.2$ V), moderate ($0.2 > E_{p/2} > 1$ V) and very weak or inactive (>1 V). Thus, at pH 7.0 DHS (E_1 peak, $E_{p/2} = 0.27$ V; E_2 peak, $E_{p/2} = 0.41$ V; vs SCE) and SIL (E_2 peak, $E_{p/2} = 0.39$ V; vs SCE) are both moderate antioxidants. The reducing properties of flavonoids are very often characterized by formal redox potentials ($E^{\circ\prime}$) determined at pH 7.0 vs normal hydrogen electrode (NHE). This parameter can be quite accurately approximated by a half-wave potential ($E_{1/2}$). We recalculated the data for SIL and DHS recorded at 5 mV s^{-1}, knowing that $E_{p/2}$ precedes $E_{1/2}$ by 28/n mV.[82] The results are presented in Table 3, and for SIL they are in good agreement

Table 3. Formal Redox Potentials at pH 7.0 vs NHE for DHS, SIL, and Some Oxygen-Centered Radicals

redox couple	$E^{\circ\prime}$/V
DHS$_{ox}$/DHS$_{red}$ (3-OH and 20-OH sites)	0.53; 0.68[a]
SIL$_{ox}$/SIL$_{red}$ (20-OH site)	0.66[a]
ROO$^{\bullet}$, H^{+}/ROOH	0.77–1.44[b]
O$_2^{\bullet-}$, 2H^{+}/H$_2$O$_2$	0.94[b]
HO$_2^{\bullet}$, H^{+}/H$_2$O$_2$	1.06[b]
OH$^{\bullet}$, H^{+}/H$_2$O	2.31[b]

[a]This work. [b]Reference 83.

with $E^{\circ\prime}$ obtained previously by Gyorgy et al. (0.62 and 0.76 V[80] vs NHE). In comparison with the redox potentials of reactive

oxygen species such as alkylperoxyl (ROO•), superoxide (O₂•⁻), hydroperoxyl (HO₂•), and hydroxyl (OH•) radicals, both SIL and DHS are able to reduce these four radicals. Moreover, DHS exhibits a redox potential similar to that of α-tocopherol (0.50 V),[83] which is one of the strongest chain-breaking antioxidants.
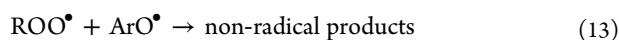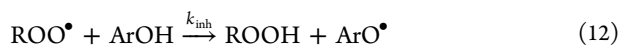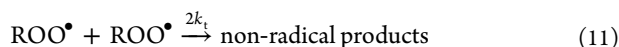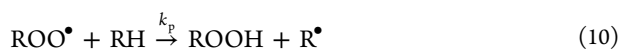
We calculated the number of electrons, n_e, participating in the oxidation processes of SIL and DHS from the equation

$$E_p - E_{p/2} = \frac{56.5 \text{ mV}}{n_e} \qquad (7)$$

where E_p is the peak potential. The values of $E_p - E_{p/2}$ at pH 4.0 are 57 mV for the E_2 peak for SIL and 34 and 57 mV for the E_1 and E_2 peaks, respectively, for DHS. That confirms one-electron oxidation at the 20-OH site in SIL, reported previously by Gyorgy et al.,[36] and also indicates the same mechanism for the 20-OH site in DHS. The E_1 peak represents a two-electron-oxidation process (a slight deviation from 28 mV might be caused by kinetic effects), and we expect that it is a more complex process due to the conjugation of rings A, C, and B. The mechanism might include one-electron/one-proton transfer from the 3-OH site followed by a change of electron density in rings A and C and/or cleavage of ring C and subsequent electron/proton transfer, similarly to electrooxidation of ring C in quercetin.[84]

The electrochemical behavior of SIL and DHS is strongly dependent on pH. In the whole pH range DHS is oxidized at lower potentials than SIL (see Figure 1B), in agreement with the better antiradical properties of DHS over SIL, observed during kinetic measurements (reaction with dpph• radical). The Nernstian slopes of $E_{p/2}$ vs pH, i.e. 58 (E_2) mV pH⁻¹ for SIL and 56 (E_2) and 59 (E_1) mV pH⁻¹ for DHS, indicate a 1:1 stoichiometry of electron transfer to proton transfer. Deviations from the Nernstian slope observed at pH ≥8.0 suggest a change in the reaction mechanism. The most significant changes occur for DHS, and at pH 8−10 we could distinguish two peaks (E_{1a} and E_{1b}) instead of one (E_1) present at lower pH. The origin of this behavior is not clear at the present stage of the study. Most likely it is related to the transition from concerted to stepwise two electron electrode process but the occurrence of two slightly different forms of DHS anions cannot be excluded. Perhaps, the bifurcation derives from the occurrence of two slightly different forms of DHS anions.

Kinetics of Lipid Oxidation in Heterogeneous Systems. We investigated the antioxidant activities of SIL and DHS during peroxidation (reactions 8−13) of methyl linoleate

$$RH \xrightarrow{R_i} R^\bullet \qquad (8)$$

$$R^\bullet + O_2 \rightarrow ROO^\bullet \qquad (9)$$

$$ROO^\bullet + RH \xrightarrow{k_p} ROOH + R^\bullet \qquad (10)$$

$$ROO^\bullet + ROO^\bullet \xrightarrow{2k_t} \text{non-radical products} \qquad (11)$$

$$ROO^\bullet + ArOH \xrightarrow{k_{inh}} ROOH + ArO^\bullet \qquad (12)$$

$$ROO^\bullet + ArO^\bullet \rightarrow \text{non-radical products} \qquad (13)$$

(ML) at 37 °C in Triton X-100 micelles—the system mimicking the amphiphilic environment of phospholipid bilayers. The reaction was followed by monitoring the consumption of oxygen, as the rate of oxygen uptake reflects well the rate of peroxidation process.[85]

The oxidation chain was initiated by a water-soluble azo compound 2,2′-azobis(amidinepropane) dihydrochloride (ABAP).[86] We determined the rates of initiation (R_i, reaction 8) over the pH range 4−10 using the method of Boozer et al.[87] (see the Supporting Information) for 2,2,5,7,8-pentamethyl-6-chromanol (PMHC), known to trap two peroxyl radicals by each of its molecules (stoichiometric factor $n = 2$). The values of R_i were calculated from the equation

$$R_i = \frac{n[ArOH]_0}{\tau_{ind}} \qquad (14)$$

where $[ArOH]_0$ is the initial concentration of the chain-breaking antioxidant and τ_{ind} is the length of the induction period (when consumption of oxygen is very slow). The determined rates of initiation were nearly constant 5.64 ± 0.21 nM s⁻¹ at pH 4−8 and increased only slightly to 6.55 ± 0.07 nM s⁻¹ at pH 9−10; hence, the changes in the peroxidation kinetics in this range of pH can be considered as not dependent on the R_i parameter. The experimental oxygen uptake plots for uninhibited and inhibited peroxidations are shown in Figure 2, and the corresponding data are reported in Table 4.
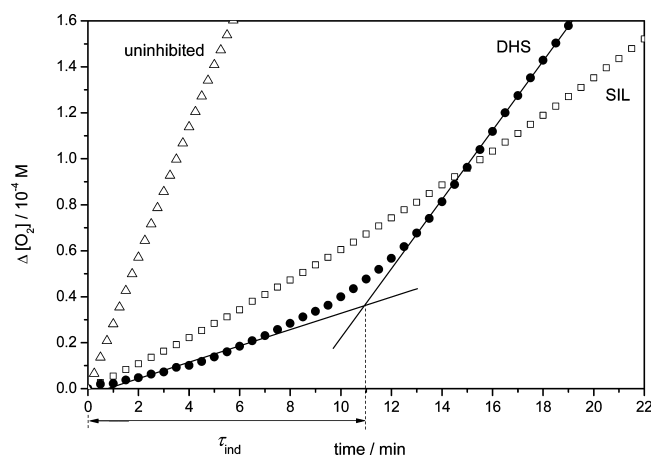

Figure 2. Oxygen uptake traces recorded during ABAP-initiated peroxidation of ML in Triton X-100 micelles at 37 °C in the absence (uninhibited) and presence of SIL (10 μM) or DHS (10 μM) at pH 8.0. For DHS a graphical method used for determination of τ_{ind} is depicted.

We observed a significant decrease in the rate of ML oxidation after addition of SIL (see R_{ABAP} and R_{ox1} in Table 4); however, we were not able to distinguish a definite induction period at any pH. This behavior is characteristic for the retardation process, which prevents the introduction of chain-initiating radicals.[88] The effect does not depend on pH for SIL. Even stronger retardation effect is observed for DHS in the pH range 4.0−6.0. At pH 7.0 its antioxidant activity undergoes a sudden increase, showing a substantial induction period, though with further increase of pH it gradually decreases, with increasing rate of inhibited peroxidation R_{inh} and kinetic chain length ν_{inh}.

The rate constant k_{inh} for the reaction 12 can be determined for the peroxidation processes that show induction period. Knowing the rate of inhibited oxygen consumption ($R_{inh} = -d[O_2]/dt$) and the propagation constant k_p[89] of ML, we calculated k_{inh} from the integrated equation[61,89−91]

$$\Delta[O_2]_t = -\frac{k_p[ML]}{k_{inh}} \ln\left(1 - \frac{t}{\tau_{ind}}\right) \qquad (15)$$

Table 4. Kinetic Parameters for the Peroxidation of 2.74 mM ML Initiated by 10 mM ABAP and Inhibited by 10 μM SIL or 10 μM DHS: Induction Time (τ_{ind}), Bimolecular Rate Constant of Reaction with Peroxyl Radicals (k_{inh}), Rate of Inhibition (R_{inh}), Rate of Oxidation When No Induction Period Is Observed (R_{ox1}) or after the Induction Period Is Over (R_{ox2}), and Kinetic Chain Length during the Induction Period (ν_{inh}), When No Induction Period Is Observed (ν_{ox1}), or after the Induction Period Is Over (ν_{ox2})

| | uninhibited | 10 μM SIL | | 10 μM DHS | | | | | | |
pH	$10^8 R_{ABAP}{}^a$/M s⁻¹	$10^8 R_{ox1}{}^b$/M s⁻¹	$\nu_{ox1}{}^c$	τ_{ind}/min	$10^8 R_{inh}$/M s⁻¹	$\nu_{inh}{}^c$	$10^{-3}k_{inh}{}^d$/M⁻¹ s⁻¹	$(10^8 R_{ox1})^b$ $10^8 R_{ox2}$/M s⁻¹	(ν_{ox1}) $\nu_{ox2}{}^c$
4	50	9.1	15					(7.8)	(13)
5	46	13	24					(10)	(18)
6	46	14	25					(8.3)	(15)
7	47	13	25	18	6.5	12	2.4	13	25
8	44	13	23	11	8.1	14	4.0	28	49
9	53	13	20	7.4	10	15	4.8	40	61
10	49	13	19	3.5	15	24	5.7	70	106

^{a}Rate of uninhibited peroxidation initiated with ABAP. ^{b}Rate of retardation. ^{c}Calculated as $\nu_{ox1} = R_{ox1}/R_i$, $\nu_{inh} = R_{inh}/R_i$, and $\nu_{ox2} = R_{ox2}/R_i$, where R_i is the rate of initiation by 10 mM ABAP. ^{d}Calculated from eq 15 with the value of $k_p = 37$ M⁻¹ s⁻¹ taken from reference 89.
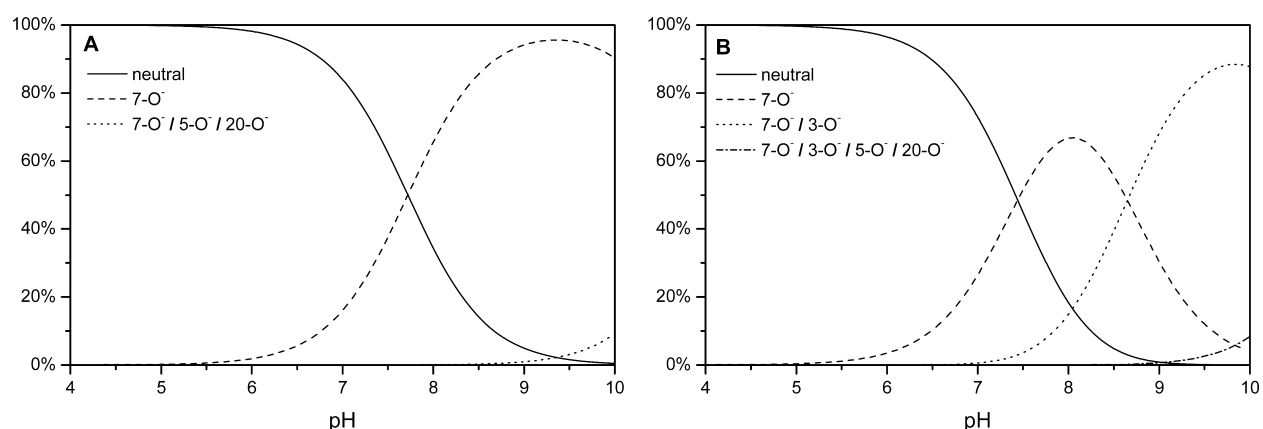

Figure 3. Dissociation diagrams of SIL (A) and DHS (B) within the pH range 4−10.

Because the reactivity of SIL does not change with increase in pH from 7.0 to 10.0 (see Table 4), we might assume that deprotonation (Figure 3A) has little or no influence on its reaction with free radicals. In the same pH range more than 2-fold acceleration of the reaction between DHS and ROO• radicals is observed (see k_{inh} in Table 4). This result is in very good agreement with our findings from the kinetic measurements with dpph• radical. Therefore, the behavior of DHS can be ascribed to the presence of the 3-OH enolic group: the induction period appears at pH 7.0, where the 3-O⁻ species constitutes 0.59% of the total DHS concentration (see Figure 3B). The increase of k_{inh} at higher pH's is consistent with the greater participation of 3-O⁻ species in overall concentration (up to 88% at pH 10.0) and, thus, enhanced SPLET participation.

Surprisingly, although the reaction of DHS and ROO• accelerates with increasing pH, other parameters (τ_{ind}, R_{inh}, ν_{inh}) seem to indicate slightly less efficacy of DHS. Perhaps, the localization of DHS molecules in the lipid/water system is responsible for this phenomenon. We calculated the distribution coefficient D of DHS using software by Hilal et al.[92] At pH 7.0 the concentration of DHS in the lipid phase is 700 times greater than in water, while at pH 10.0 it is 4 times lower than in water. On the basis of the change of distribution of DHS and the concentration and aggregation number of Triton X-100 (143 molecules per aggregate[93]), we estimated that, with pH rising from 7.0 to 10.0, the amount of DHS molecules per micelle decreases 5 times, which corresponds very well with the 5-fold decrease in induction time within this pH range and

might explain the diminished protection against peroxidation. After the antioxidant is exhausted in the inhibition process, the rate of peroxidation should be the same as the rate of the uninhibited process (R_{ABAP}). For DHS, there is a clear retarding behavior after the end of the induction period at pH 7.0 ($R_{ox2} \ll R_{ABAP}$), gradually declining as the pH increases up to pH 9.0. At pH 10.0 the effect becomes prooxidative ($R_{ox2} \gg R_{ABAP}$). These deviations can be ascribed to the retarding activity of the phenol present in the polar phase or to the fate of the phenoxyl radicals. Taking all parameters into consideration, DHS exhibits the best antioxidant activity at pH 7.0, which is a value close to the intracellular pH of hepatic cells.[94]

CONCLUSIONS

We investigated the antioxidant activity of silybin and 2,3-dehydrosilybin in several organic solvents and in a model micellar system. On the basis of kinetic considerations and acidity measurements, we found that the mechanism of action of both flavolignans depends on the environment. However, the media-dependent mechanism is limited to phenolic (enolic) groups at positions 3 and 7 in DHS and position 7 in SIL, having sufficient acidity for SPLET to occur. Other phenolic groups, namely 20-OH and 5-OH, react mostly via a HAT mechanism because of their higher pK_a. Their reaction via SPLET is possible in solvents highly supporting ionization/at very high pH; however, at physiologically relevant pH's this mechanism is negligible. Kinetics and electrochemical data indicate that DHS is a much better radical scavenger than SIL

in all studied systems. This is due to the presence of the enolic 3-OH group conjugated with the C2−C3 double bond and C4 carbonyl group. The radical formed at this site is relatively stable, as the electron is delocalized over three flavone rings. The participation of 3-OH group is favored in both mechanisms, HAT (lowest $BDE_{O−H}$) and SPLET (moderate acidity), and provides enhanced antioxidant activity of DHS. Studies in a lipid/water system suggest that the partition of the chain-breaking antioxidant between two phases is an important factor controlling its antioxidant behavior. While the reaction with peroxyl radicals accelerates with rising pH due to an increase in SPLET participation, the decrease in the number of molecules in the lipid phase impairs its protection against peroxidation processes.

■ EXPERIMENTAL SECTION

Materials. All chemicals used in the experiments were of the highest purity and are commercially available, except for 2,3-dehydrosilybin, which was prepared from silybin as described by Maitrejean et al.[95] ¹H NMR spectra of DHS were recorded in acetone at 200 MHz and DMSO at 500 MHz (COSY) with TMS as an internal standard. Chemical shifts (δ) are given in parts per million and coupling constants (J) in hertz (Hz). Melting point was measured on a melting point apparatus.

2,3-Dehydrosilybin. Light yellow powder, mp 228−233 °C. ¹H NMR (acetone-d_6, 200 MHz, 22 °C): 3.57 (1H, m, H-23(1)), 3.79 (1H, m, H-23(2)), 3.90 (3H, s, OCH₃), 4.26 (1H, m, H-10), 5.07 (1H, d, J = 8.1, H-11), 6.28 (1H, d, J = 2.1, H-6), 6.59 (1H, d, J = 2.1, H-8), 6.91 (1H, d, J = 8.1, H-21), 6.93 (1H, s, H-18), 7.02 (1H, dd, J = 8.2, 2.0, H-22), 7.10 (1H, d, J = 9.2, H-16), 7.85 (1H, m, H-15), 7.88 (1H, m, H-13), 9.71 (1H, s, 20-OH), 12.15 (1H, s, 5-OH). ¹H NMR (DMSO-d_6, 500 MHz, 25 °C): 3.36 (1H, m, H-23(1)), 3.57 (1H, m, H-23(2)), 3.79 (3H, s, OCH₃), 4.27 (1H, m, H-10), 4.96 (1H, d, J = 7.9, H-11), 4.99 (1H, m, 23-OH), 6.19 (1H, d, J = 2.1, H-6), 6.46 (1H, d, J = 2.1, H-8), 6.81 (1H, d, J = 8.1, H-21), 6.89 (1H, dd, J = 8.1, 1.9, H-22), 7.04 (1H, d, J = 1.9, H-18), 7.12 (1H, d, J = 9.0, H-16), 7.74 (1H, d, J = 2.2, H-13), 7.77 (1H, m, H-15), 9.16 (1H, s, 20-OH), 9.56 (1H, s, 3-OH), 10.81 (1H, s, 7-OH), 12.41 (1H, s, 5-OH). MS-ESI (m/z): $[M + H]^+$ calcd for $C_{25}H_{21}O_{10}$ 481.43, found 481.1; $[M + Na]^+$ calcd for $C_{25}H_{20}O_{10}Na$ 503.41, found 503.1.

pK_a Measurements. The values of pK_a for SIL and DHS in water/methanol (1/1) were determined as described previously.[47] Briefly, samples of flavonolignan solution at a concentration of 8×10^{-5} M in water/methanol were titrated with 1 M KOH and the process was monitored with a precision pH meter with a combined pH glass electrode. The UV−vis spectrometer was employed to record the spectra within the range 200−600 nm over a pH range of 1.5−13.5 (corrected for the water/methanol system). Obtained data were processed with Datan 3.0 software.

Kinetic Measurements. The kinetics of the reaction of SIL and DHS with dpph• was measured by the stopped-flow method as described previously.[47] Measurements were conducted in solvents of different polarity and H-bond basicity: i.e. dioxane, methanol, acidified methanol, ethyl acetate, acetate buffer (pH 5.5), and Tris buffer (pH 7.4). A decrease of dpph• ($(2−11) \times 10^{-5}$ M) absorbance at 517 nm in the presence of an excess of the phenols was monitored by a UV−vis spectrophotometer connected to a single-mixing stopped-flow system. With constant [dpph•] and various [PhOH] a series of pseudo-first-order rate constants (k_{exp}) was calculated as average values from at least two independent sets of measurements. Values of the bimolecular rate constants (k^S) were obtained as a slope of the straight-line equation $k_{exp} = k^S[PhOH]$ + constant.

Cyclic Voltammetry. Measurements were carried out in a three-electrode system; the saturated (Hg|Hg₂SO₄|K₂SO₄) mercury sulfate reference electrode was separated from the studied solution with a salt bridge. An Au wire with a large surface area (ca. 5 cm²) served as a counter electrode. As the working electrode a glassy-carbon disk embedded in Teflon with a surface area exposed to the solution of A = 0.031 cm² was used. The electrode surface was polished with alumina

paste (Buehler, 5, 1, and 0.05 μm), rinsed with deionized water, and immersed into an ultrasonic bath to remove residual alumina. This procedure was repeated prior to each voltammetry experiment, in which only one potential scan cycle was registered with scan rate ν = 0.05 or 0.005 V s⁻¹. The acidity of the solution was determined by using a pH glass electrode. The pH was adjusted using an automatic titrator within the range 4−10 (with a step of 1). The measurements were performed at room temperature in 10 mL of modified Britton−Robinson buffer (pH 10, titration with 85% H₃PO₄) in the absence and in the presence of SIL or DHS. A stock solution of the compound in methanol (1−2 mg/mL) was added to the buffer solution at pH 10 to obtain an initial concentration of 1×10^{-4} M. The solution was deoxygenated with an Ar flow. The half-peak oxidation potentials ($E_{p/2}$) were determined.

Oxygen Uptake Measurements. The oxygen depletion during autoxidation of methyl linoleate (2.7 mM) was measured in Triton X-100 emulsions at 37 °C in the absence and presence of SIL or DHS over a pH range of 4−10. The pH's of all samples were maintained using series of buffers: acetate buffer (pH 4−5), phosphate buffer (pH 6−8), and borate buffer (pH 9−10). A Biological Oxygen Monitor equipped with a Clark-type electrode was used to follow the oxidation course. Each sample (5.0 mL) was first saturated with oxygen in a measuring chamber equipped with a magnetic stirring disk, the electrode was placed in the chamber, and then autoxidation was initiated by the injection of 2,2′-azobis(2-amidinopropane) hydrochloride (ABAP) solution to obtain 10 mM final concentration. After the level of oxygen decreased by 10%, 10 μL of a stock solution of flavonolignan in methanol was injected, without opening the chamber, to obtain 10 μM final concentration. A 1% amount of oxygen depletion recorded refers to 2.2×10^{-6} M of oxygen consumed (see the Supporting Information). The rates of inhibited and noninhibited autoxidations were determined from the slopes of oxygen uptake. The length of induction periods was determined graphically as the time between antioxidant injection and the point of intersection of tangents to parts of the curve representing the inhibited oxidation and final uninhibited oxidation (see Figure 2 in the text).

■ ASSOCIATED CONTENT

⑤ Supporting Information

Figures and tables giving ¹H NMR (1D and 2D) and MS ESI spectra of DHS, UV−vis titration spectra for SIL and DHS, detailed kinetic data for reactions of the (poly)phenols with dpph• in neat solvents, acidified methanol, and buffered solutions, half-peak potentials for SIL and DHS at scan speeds of 5 and 50 mV s⁻¹, rates of initiation of ABAP-initiated peroxidation, a plot of oxygen depletion against $-\ln(1 − t/\tau)$, and details of the calculation of O₂ molar concentration in the micellar system. This material is available free of charge via the Internet at http://pubs.acs.org.

■ AUTHOR INFORMATION

Corresponding Author
*E-mail: litwin@chem.uw.edu.pl

Notes
The authors declare no competing financial interest.

■ ACKNOWLEDGMENTS

■ REFERENCES

(1) De Smet, P. A. G. M. *Drugs* **1997**, *54*, 801−840.
(2) Fabricant, D. S.; Farnsworth, N. R. *Environ. Health. Perspect.* **2001**, *109*, 69−75.

(3) Farnsworth, N. R.; Akerele, O.; Bingel, A. S.; Soejarto, D. D.; Guo, Z. *Bull. W. H. O.* **1985**, *63*, 965−981.

(4) Vane, J. R.; Botting, R. M. *Thromb. Res.* **2003**, *110*, 255−258.

(5) Hanks, G. W.; de Conno, F.; Cherny, N.; Hanna, M.; Kalso, E.; McQuay, H. J.; Mercadante, S.; Meynadier, J.; Poulain, P.; Ripamonti, C.; Radbruch, L.; Roca i Casas, J.; Sawe, J.; Twycross, R. G.; Ventafridda, V. *Br. J. Cancer* **2001**, *84*, 587−593.

(6) Krishna, S.; White, N. J. *Clin. Pharmacokinet.* **1996**, *30*, 263−299.

(7) Ye, K.; Ke, Y.; Keshava, N.; Shanks, J.; Kapp, J. A.; Tekmal, R. R.; Petros, J.; Joshi, H. C. *Proc. Natl. Acad. Sci. U. S. A.* **1998**, *95*, 1601−1606.

(8) Aggarwal, B. B.; Sundaram, C.; Malani, N.; Ichikawa, H. *Adv. Exp. Med. Biol.* **2007**, *595*, 1−75.

(9) Ferguson, D. W.; Berg, W. J.; Sanders, J. S.; Roach, P. J.; Kempf, J. S.; Kienzle, M. G. *Circulation* **1989**, *80*, 65−77.

(10) Ang-Lee, M. K.; Moss, J.; Yuan, C.-S. *J. Am. Med. Assoc.* **2001**, *286*, 208−216.

(11) De Smet, P. A. G. M. *New Engl. J. Med.* **2002**, *347*, 2046−2056.

(12) *Modern Phytomedicine. Turning Medicinal Plants into Drugs*; Ahmad, I., Aquil, F., Owais, M., Eds.; Wiley-VCH: Weinheim, Germany, 2006.

(13) Abenavoli, L.; Capasso, R.; Milic, N.; Capasso, F. *Phytother. Res.* **2010**, *24*, 1423−1432.

(14) Ferenci, P.; Dragosics, B.; Dittrich, H.; Frank, H.; Benda, L.; Lochs, H.; Meryn, S.; Base, W.; Schneider, B. *J. Hepatol.* **1989**, *9*, 105−113.

(15) Mayer, K. É.; Myers, R. P.; Lee, S. S. *J. Viral Hepatitis* **2005**, *12*, 559−567.

(16) Poucheret, P.; Fons, F.; Dore, J. C.; Michelot, D.; Rapior, S. *Toxicon* **2010**, *55*, 1338−1345.

(17) Ruan, X.; Shen, C.; Meng, Q. *Food Chem. Toxicol.* **2010**, *48*, 1145−1151.

(18) Wellington, K.; Jarvis, B. *BioDrugs* **2001**, *15*, 465−489.

(19) Crocenzi, F. A.; Roma, M. G. *Curr. Med. Chem.* **2006**, *13*, 1055−1074.

(20) Deep, G.; Agarwal, R. *Cancer Metastasis Rev.* **2010**, *29*, 447−463.

(21) Gazak, R.; Walterova, D.; Kren, V. *Curr. Med. Chem.* **2007**, *14*, 315−338.

(22) Yin, F.; Liu, J.; Ji, X.; Wang, Y.; Zidichouski, J.; Zhang, J. *Neurochem. Int.* **2011**, *58*, 399−403.

(23) Trouillas, P.; Marsal, P.; Svobodova, A.; Vostalova, J.; Gazak, R.; Hrbac, J.; Sedmera, P.; Kren, V.; Lazzaroni, R.; Duroux, J.-L.; Walterova, D. *J. Phys. Chem. A* **2008**, *112*, 1054−1063.

(24) Carini, R.; Comoglio, A.; Albano, E.; Poli, G. *Biochem. Pharmacol.* **1992**, *43*, 2111−2115.

(25) Gazak, R.; Sedmera, P.; Vrbacky, M.; Vostalova, J.; Drahota, Z.; Marhol, P.; Walterova, D.; Kren, V. *Free Radical Biol. Med.* **2009**, *46*, 745−758.

(26) Gazak, R.; Svobodova, A.; Psotova, J.; Sedmera, P.; Prikrylova, V.; Walterova, D.; Kren, V. *Bioorg. Med. Chem.* **2004**, *12*, 5677−5687.

(27) Kosina, P.; Kren, V.; Gebhardt, R.; Grambal, F.; Ulrichova, J.; Walterova, D. *Phytother. Res.* **2002**, *16*, S33−39.

(28) Pietrangelo, A.; Borella, F.; Casalgrandi, G.; Montosi, G.; Ceccarelli, D.; Gallesi, D.; Giovannini, F.; Gasparetto, A.; Masini, A. *Gastroenterology* **1995**, *109*, 1941−1949.

(29) Skottova, N.; Krecman, V.; Simanek, V. *Phytother. Res.* **1999**, *13*, 535−537.

(30) Machicao, F.; Sonnenbichler, J. *Hoppe-Seyler's Z. Physiol. Chem.* **1977**, *358*, 141−147.

(31) Fraschini, F.; Demartini, G.; Esposti, D. *Clin. Drug Invest.* **2002**, *22*, 51−65.

(32) Trost, W.; Halbach, G. *Experientia* **1978**, *34*, 1051−1052.

(33) Valenzuela, A.; Garrido, A. *Biol. Res.* **1994**, *27*, 105−112.

(34) Huber, A.; Thongphasuk, P.; Erben, G.; Lehmann, W.-D.; Tuma, S.; Stremmel, W.; Chamulitrat, W. *Biochim. Biophys. Acta* **2008**, *1780*, 837−847.

(35) Loguercio, C.; Festi, D. *World J. Gastroenterol.* **2011**, *17*, 2288−2301.

(36) Gyorgy, I.; Antus, S.; Foldiak, G. *Radiat. Phys. Chem.* **1992**, *39*, 81−84.

(37) Foti, M. C. *J. Pharm. Pharmacol.* **2007**, *59*, 1673−1685.

(38) Foti, M. C.; Amorati, R. *J. Pharm. Pharmacol.* **2009**, *61*, 1435−1448.

(39) Leon-Carmona, J. R.; Alvarez-Idaboy, J. R.; Galano, A. *Phys. Chem. Chem. Phys.* **2012**, *14*, 12534−12543.

(40) Mayer, J. M.; Hrovat, D. A.; Thomas, J. L.; Borden, W. T. *J. Am. Chem. Soc.* **2002**, *124*, 11142−11147.

(41) Litwinienko, G.; Ingold, K. U. *Acc. Chem. Res.* **2007**, *40*, 222−230.

(42) HAT refers to a transfer of the proton and the electron together, as a hydrogen atom. PCET is usually considered as a transfer of the proton and electron between different sets of orbitals; however, there is no universally recognized definition of PCET. Since the magnitude of the Kinetic Solvent Effect is the same for both mechanisms, we use a general HAT notation.[40,41]

(43) Litwinienko, G.; Ingold, K. U. *J. Org. Chem.* **2004**, *69*, 5888−5896.

(44) Foti, M. C.; Daquino, C.; Geraci, C. *J. Org. Chem.* **2004**, *69*, 2309−2314.

(45) Galano, A.; Leon-Carmona, J. R.; Alvarez-Idaboy, J. R. *J. Phys. Chem. B* **2012**, *116*, 7129−7137.

(46) Kosinova, P.; Gazak, R.; Duroux, J.-L.; Lazzaroni, R.; Kren, V.; Assfeld, X.; Trouillas, P. *ChemPhysChem* **2011**, *12*, 1135−1142.

(47) Musialik, M.; Kuzmicz, R.; Pawlowski, T. S.; Litwinienko, G. *J. Org. Chem.* **2009**, *74*, 2699−2709.

(48) Agrawal, P. K.; Schneider, H.-J. *Tetrahedron Lett.* **1983**, *24*, 177−180.

(49) Wolfbeis, O. S.; Leiner, M.; Hochmuth, P.; Geiger, H. *Ber. Bunsen-Ges. Phys. Chem.* **1984**, *88*, 759−767.

(50) Meloun, M.; Burkonova, D.; Syrovy, T.; Vrana, A. *Anal. Chim. Acta* **2003**, *486*, 125−141.

(51) Smiths, M. B.; March, J. *March's Advanced Organic Chemistry*, 5th ed.; Wiley: New York, 2001.

(52) Magnusson, L. B.; Postmus, C.; Craig, C. A. *J. Am. Chem. Soc.* **1963**, *85*, 1711−1715.

(53) Sergeant, E. P.; Dempsey, B. *Ionization constants of organic acids in aqueous solution*; Pergamon Press: Oxford, U.K., 1979.

(54) Snelgrove, D. W.; Lusztyk, J.; Banks, J. T.; Mulder, P.; Ingold, K. U. *J. Am. Chem. Soc.* **2001**, *123*, 469−477.

(55) Abraham, M. H.; Grellier, P. L.; Prior, D. V.; Morris, J. J.; Taylor, P. J. *J. Chem. Soc., Perkin Trans. 2* **1990**, 521−529.

(56) Abraham, M. H.; Grellier, P. L.; Prior, D. V.; Duce, P. P.; Morris, J. J.; Taylor, P. J. *J. Chem. Soc., Perkin Trans. 2* **1989**, 699−711.

(57) Foti, M.; Ruberto, G. *J. Agric. Food Chem.* **2001**, *49*, 342−348.

(58) MacFaul, P. A.; Ingold, K. U.; Lusztyk, J. *J. Org. Chem.* **1996**, *61*, 1316−1321.

(59) Litwinienko, G.; Ingold, K. U. *J. Org. Chem.* **2003**, *68*, 3433−3438.

(60) Musialik, M.; Litwinienko, G. *Org. Lett.* **2005**, *7*, 4951−4954.

(61) Foti, M. C.; Johnson, E. R.; Vinqvist, M. R.; Wright, J. S.; Barclay, L. R. C.; Ingold, K. U. *J. Org. Chem.* **2002**, *67*, 5190−5196.

(62) Foti, M. C.; Daquino, C. *Chem. Commun.* **2006**, 3252−3254.

(63) The value of 0.41 reported by Abraham et al.[55] is not statistically corrected for the presence of two easily accessible HB sites in one molecule of dioxane. The experimental value of 0.47 was determined for dioxane by infrared spectroscopic methods.[43] Thus, 1,4-dioxane is a better HB acceptor than ethyl acetate. This is in agreement with slower HAT reactions in dioxane in comparison to ethyl acetate.

(64) Amic, D.; Lucic, B. *Bioorg. Med. Chem.* **2010**, *18*, 28−35.

(65) Heijnen, C. G. M.; Haenen, G. R. M. M.; Oostveen, R. M.; Stalpers, E. M.; Bast, A. *Free Radical Res.* **2002**, *36*, 575−581.

(66) Ishiki, H. M.; Donate, P. M.; Galembeck, S. E. *J. Mol. Struct. (THEOCHEM)* **1998**, *423*, 235−243.

(67) Matos, M. A. R.; Sousa, C. C. S.; Miranda, M. S.; Morais, V. M. F.; Liebman, J. F. *J. Phys. Chem. B* **2009**, *113*, 11216−11221.

(68) Polly, R.; Taylor, P. R. *J. Phys. Chem. A* **1999**, *103*, 10343−10347.

(69) Hayashi, T.; Kawai, S.; Ohno, T. *Chem. Pharm. Bull.* **1971**, *19*, 792−795.

(70) Binbuga, N.; Schultz, T. P.; Henry, W. P. *Tetrahedron Lett.* **2008**, *49*, 5762−5765.

(71) Anouar, E. H.; Gierschner, J.; Duroux, J.-L.; Trouillas, P. *Food Chem.* **2012**, *131*, 79−89.

(72) Trouillas, P.; Marsal, P.; Siri, D.; Lazzaroni, R.; Duroux, J.-L. *Food Chem.* **2006**, *97*, 679−688.

(73) van Acker, S. A. B. E.; de Groot, M. J.; van den Berg, D.-J.; Tromp, M. N. J. L.; Donne-Op den Kelder, G.; van der Vijgh, W. J. F.; Bast, A. *Chem. Res. Toxicol.* **1996**, *9*, 1305−1312.

(74) Foti, M.; Piattelli, M.; Baratta, M. T.; Ruberto, G. *J. Agric. Food Chem.* **1996**, *44*, 497−501.

(75) Tian, Y.-X.; Han, R.-M.; Fu, L.-M.; Zhang, J.-P.; Skibsted, L. H. *J. Phys. Chem. B* **2008**, *112*, 2273−2280.

(76) Han, R.-M.; Tian, Y.-X.; Liu, Y.; Chen, C.-H.; Ai, X.-C.; Zhang, J.-P.; Skibsted, L. H. *J. Agric. Food Chem.* **2009**, *57*, 3780−3785.

(77) Rice-Evans, C. A.; Miller, N. J.; Paganga, G. *Free Radical Biol. Med.* **1996**, *20*, 933−956.

(78) Heim, K. E.; Tagliaferro, A. R.; Bobilya, D. J. *J. Nutr. Biochem.* **2002**, *13*, 572−584.

(79) Bors, W.; Heller, W.; Michel, C.; Saran, M. *Methods Enzymol.* **1990**, *186*, 343−355.

(80) Gyorgy, I.; Antus, S.; Blazovics, A.; Foldiak, G. *Int. J. Radiat. Biol.* **1992**, *61*, 603−609.

(81) van Acker, S. A. B. E.; van den Berg, D.-J.; Tromp, M. N. J. L.; Griffioen, D. H.; van Bennekom, W. P.; van der Vijgh, W. J. F.; Bast, A. *Free Radical Biol. Med.* **1996**, *20*, 331−342.

(82) Nicholson, R. S.; Shain, I. *Anal. Chem.* **1964**, *36*, 706−723.

(83) Halliwell, B.; Gutteridge, J. M. C. *Free Radicals in Biology and Medicine*, 4th ed.; Oxford University Press: New York, 2007.

(84) Jorgensen, L. V.; Cornett, C.; Justesen, U.; Skibsted, L. H.; Dragsted, L. O. *Free Radical Res.* **1998**, *29*, 339−350.

(85) Yamamoto, Y.; Niki, E.; Kamiya, Y. *Bull. Chem. Soc. Jpn.* **1982**, *55*, 1548−1550.

(86) Musialik, M.; Kita, M.; Litwinienko, G. *Org. Biomol. Chem.* **2008**, *6*, 677−681.

(87) Boozer, C. E.; Hammond, G. S.; Hamilton, C. E.; Sen, J. N. *J. Am. Chem. Soc.* **1955**, *77*, 3233−3237.

(88) Marcuse, R.; Fredriksson, P.-O. *J. Am. Oil Chem. Soc.* **1969**, *46*, 262−268.

(89) Pryor, W. A.; Strickland, T.; Church, D. F. *J. Am. Chem. Soc.* **1988**, *110*, 2224−2229.

(90) Burton, G. W.; Ingold, K. U. *J. Am. Chem. Soc.* **1981**, *103*, 6472−6477.

(91) Lucarini, M.; Pedulli, G. F. *Chem. Soc. Rev.* **2010**, *39*, 2106−2119.

(92) Hilal, S. H.; Karickhoff, S. W.; Carreira, L. A. *QSAR Comb. Sci.* **2004**, *23*, 709−720.

(93) Robson, R. J.; Dennis, E. A. *J. Phys. Chem.* **1977**, *81*, 1075−1078.

(94) Di Sario, A.; Baroni, G. S.; Bendia, E.; Ridolfi, F.; Saccomanno, S.; Ugili, L.; Trozzi, L.; Marzioni, M.; Jezequel, A. M.; Macarri, G.; Benedetti, A. *J. Hepatol.* **2001**, *34*, 378−385.

(95) Maitrejean, M.; Comte, G.; Barron, D.; El Kirat, K.; Conseil, G.; Di Pietro, A. *Bioorg. Med. Chem. Lett.* **2000**, *10*, 157−160.